

High-velocity collisions from the lunar cataclysm recorded in asteroidal meteorites

1. Interpreting ancient ^{40}Ar - ^{39}Ar ages: Are they from parent body cooling, impacts, or both?

The process or processes that created the most ancient ^{40}Ar - ^{39}Ar reset ages in stony meteorites, ranging from 4.3-4.56 Gyr ago, is currently a fascinating topic of discussion. There are two schools of thought on what happened to meteorite parent bodies at this time.

In a recent review article, (2) argued that most ordinary chondrite ^{40}Ar - ^{39}Ar ages in this interval were unlikely to have been reset by impact. Instead, he believes these ages probably reflect the closure of the ^{40}Ar - ^{39}Ar system via cooling after parent body metamorphism. In support of this, he points out that the timing of these events, many tens to a few hundreds of Myr after the formation of the first solids at ~ 4.568 Gyr ago (48), appear to broadly correspond to modeling work of the thermal evolution of chondritic parent bodies (e.g., 49). In addition, many H-chondrites appear to have cooling trends that would suggest they were produced in an undisturbed “onion-layer” system, with hotter materials in the interior cooling slowly and colder materials nearer the surface cooling more rapidly (21,50,51).

On the other hand, there is considerable evidence in the meteorite record for impacts taking place at this same time (shock veins, melt pockets, mixtures of metal and sulfides, agglutinates, etc.; 52,53). Thus, even if some meteorite parent bodies managed to go largely undisturbed from an internal thermal standpoint, their surface and upper layers were still susceptible to the effects of collisions, with impact heating and ^{40}Ar - ^{39}Ar reset age events beginning early in solar system history (e.g. 2).

As evidence, consider that several ancient impact melt clasts have been found in the L- and H-chondrites, along with some meteorites that have experienced whole-rock metamorphism (e.g., 3,40,41,54). In fact, (52) claims that about half of all of the known impact-melted ordinary chondrite materials appear to have formed > 4.4 Gyr ago. In addition, several iron meteorite groups with silicate clasts have also experienced ancient impact heating events (e.g., IAB irons, IIE irons; see 2). In terms of undisturbed onion-layer cooling for meteorite parent bodies, there is limited evidence for this beyond the H-chondrites, and even the H-chondrites themselves show signs that there was some regional mixing of petrographic types by impacts before the samples cooled below 800 K (e.g. 55,56). In fact, (56) claims that the cooling rates of brecciated and unbrecciated chondrites suggests that the H, L, and LL parent bodies were disrupted and reassembled during metamorphism.

For Vesta, the likely parent body of most HEDs, (57) find evidence in zircons derived from eucrites that energetic impact events took place several tens of Myr after Vesta differentiated. The ages of these events are similar to a narrow spike of ^{40}Ar - ^{39}Ar ages at 4.45 Gyr ago found among the unbrecciated eucrites that may also be related to at least one powerful impact event (2).

The most straightforward interpretation of the data is that parent body cooling and impacts both play a role in producing ancient ^{40}Ar - ^{39}Ar ages. This scenario is not only consistent with what we know about the thermal histories of asteroids, but also with the implications of planet formation models. Specifically, the ancient ^{40}Ar - ^{39}Ar ages take place at the same time as terrestrial planet formation, when planetary embryos and protoplanets were scattering planetesimals across the inner solar system (e.g. 13). It is almost unavoidable that some leftover planetesimals would have been scattered onto highly eccentric orbits where they could batter primordial main belt asteroids at high impact velocities. Accordingly, the ancient ^{40}Ar - ^{39}Ar ages of meteorites, if interpreted correctly, may provide critical constraints for these processes.

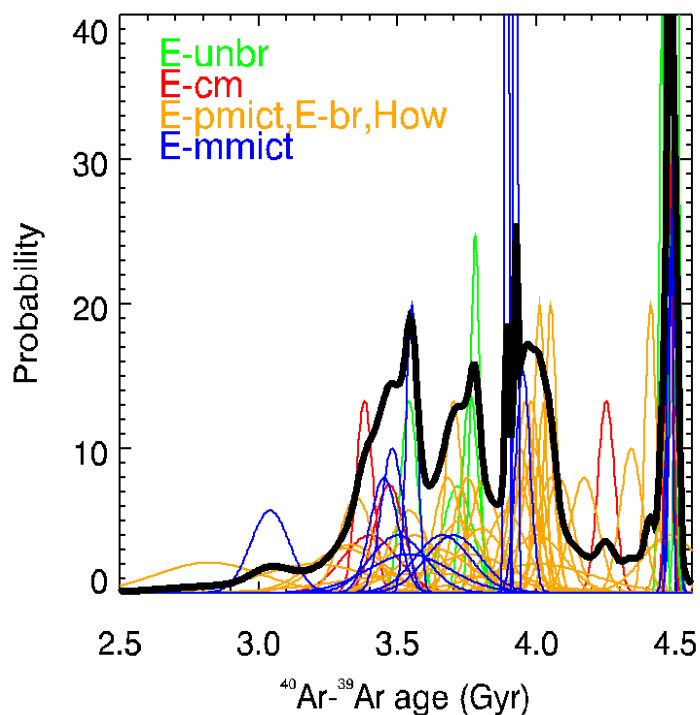
2. Eucrite and howardite petrological types and their ^{40}Ar - ^{39}Ar age ages.

Additional insights into ^{40}Ar - ^{39}Ar age reset processes on asteroids can be gleaned by examining the petrological types of the well-sampled eucrite and howardite meteorite classes (Fig. S1). The plot shows several eucrites with ages from ~ 4.45 Gyr ago, many which come from unbrecciated, cumulate and monomict eucrites. The interesting question is how these samples managed to avoid brecciation or impact alteration processes over the subsequent 4.45 Gyr ago.

It has been argued (2) (see also references therein) that a large impact on Vesta 4.45 Gyr ago would eject warm fragments into the primordial main belt, where they would undergo rapid cooling. From there, the fragments would be unlikely to undergo extensive shock heating from impacts, mainly because small bodies readily lose ejecta during impact events (e.g. 58). This scenario would also potentially explain the ancient ages and properties of the angrite meteorites (58). The issue then becomes whether these bodies can survive 4.45 Gyr ago of collisional and dynamical evolution.

A second scenario is that the ancient eucrites were reset at depth, where they could have escaped brecciation, and then were ejected by a later impact event (possibly the Rheasilvia basin formation event ~ 1 Gyr ago; 35). The process of Ar reset at depth may also have occurred in more recent times because a handful of unbrecciated eucrites have ages between 3.5-4.1 Gyr ago.

Figure S1. ^{40}Ar - ^{39}Ar ages of eucrites and howardites (see Fig. 1 for references). Each dated sample is reported with a gaussian profile with center and width corresponding to the most probable age and $1\text{-}\sigma$ error. Profiles are color coded according to the class of the parent meteorites (retrieved from the on-line Meteoritical Bulletin database, Oct. 2011): unbrecciated eucrite (E-unbr), cumulate eucrite (E-cm), polymict (E-pmict) and monomict eucrites (E-mmict), brecciated eucrite (E-br) and howardites (How). The black curve is the sum probability distribution obtained by the sum of all gaussians divided by 5. Most eucrites that show few signs of impact alteration (unbrecciated, cumulate, monomict) have ages of about 4.45 Gyr ago. Interestingly, a few have younger ages, possibly suggesting that some impacts produce heating at depth. Note also that the thermal history of the samples may affect the height of the y-axis values, but not the ages displayed on the x-axis (the same comment apply to Fig. 1).



3. On the selection effects and sampling biases of lunar and asteroid samples.

One difficulty in comparing the ^{40}Ar - ^{39}Ar ages of lunar and asteroid samples is properly accounting for selection effects and sampling biases. Consider the following issues, which is only a partial description of everything there is to think about:

→ The ^{40}Ar - ^{39}Ar ages of rocks that are indigenous to a surface can only be as old as the surface itself. Thus, if a particular region on the Moon or an asteroid is only 3 Gyr old, the ^{40}Ar - ^{39}Ar ages of rocks indigenous to that surface have to be 3 Gyr or younger. This sets limits on how the age distributions from some surfaces should be interpreted.

→ Lunar samples collected by the Apollo astronauts or the Luna spacecraft have, in some cases, an unknown origin, and may have been thrown to the collection site as ejecta. This raises the issue of whether samples are more likely to come from nearby local craters or from distant basins (and which ones). The data used in this work are from: for the Apollo 16 (85 ages) (10,59-66). For the lunar meteorites (57 ages) (4,67-71).

→ In a related manner, all of the Apollo and Luna samples were collected from the nearside of the Moon. This makes it possible that some rocks are either ejecta from or rocks affected by a few major impact events (e.g., the formation of Imbrium basin).

→ Lunar meteorites probably came from small individual cratering events that occurred very recently, according to interpretations of both their physical properties and their short cosmic-ray exposure (CRE) ages (most < 1 Myr; 43,72,73). They are thought to provide a random sample of nearside and farside terrains (4). The ^{40}Ar - ^{39}Ar ages of the impact melt clasts in lunar meteorites, however, are probably samples of much smaller impact events than those found in certain Apollo samples, which in some cases are from basin-forming events.

→ On the Moon, and perhaps on asteroids, the surface rocks are biased toward younger ejecta that happens to be on or near the surface; this allows them to be ejected by small impact events (e.g. 73). Younger ejecta buries older rocks and makes them less accessible. Moreover, older samples are more likely to be broken down and obliterated by impacts (74). This should produce a bias toward younger samples.

→ The HEDs are thought to come from the Vesta family in the main belt, most which was probably produced by the ~ 1 Gyr old Rheasilvia basin forming event (36). The immediate precursors of the HEDs are thought to arrive at Earth through a combination of a collisional cascade within the Vesta family (which creates meteoroids), Yarkovsky thermal drift processes (which transfers the meteoroids to resonances), and the effects of main belt resonances (which delivers the meteoroids to Earth-crossing orbits). This means that collisional and dynamical processes in the main belt can strongly affect what is arriving on Earth today.

→ The location of the H-chondrite parent body (HPB) is unknown but is probably located in the inner/central main belt; this is the easiest way to explain a host of constraints, including the CRE ages of the meteorites, the large fraction of meteorite falls that are H-chondrites, etc. (e.g. 75). It is plausible that the parent body hit by something big in the past, and that its meteoroids come from an H-chondrite family (76). It is also plausible that the HPB is still intact, and that the meteoroids are ejecta from cratering events on the HPB (77). The immediate precursors of the H-chondrites also have to use the same dynamical processes as the HEDs to reach Earth.

→ Most impact heating events capable of producing ^{40}Ar - ^{39}Ar ages on main belt asteroids come from highly eccentric projectiles that can strike at $V > 10$ km/s. Our work shows these events are rare, and most asteroid impacts do not produce much heating. For the Moon, however, the majority of impactors over the last 4.1 Gyr have hit at $V > 10$ km/s, with their mean impact velocities near 20 km/s (12,28). This means that the majority of lunar projectiles produce some substantial heating, though how much depends on the impactor's orbit and size. Between 4.1-4.55 Gyr ago, however, the mean impact velocity of objects striking the Moon may only have ~ 12 km/s (12,15). This difference is interesting, and might partially explain the relative paucity of ^{40}Ar - ^{39}Ar ages on the Moon older than 4.1-4.2 Gyr ago.

These factors must influence the ^{40}Ar - ^{39}Ar age distributions from Fig. 1, but how they should be weighted with respect to one another when interpreting the data is unclear. Given this, it is perhaps a surprise that the Fig. 1 distributions from the HEDs, H-chondrites, lunar meteorites, and Apollo samples are even remotely similar to one another. This may suggest that most of these selection effects and sampling biases, while important, are manageable if caution is employed and the questions asked of the data are carefully posed. For instance, a common feature of those age distributions is the presence of an uptick at about 4.1-4.2 Gyr ago (Fig. 1), although this age cannot be precisely determined given the uncertainties involved. Still, the reader should always keep in mind that these curves are constructed from a collection of impact-reset ages, and cannot be used to quantitatively estimate the impact flux. At best, they can be used to qualitatively evaluate changes in the impact flux and/or impact conditions.

To explore, at least in part, how some of the above processes may alter impact-reset age distributions, we wrote a simplistic terrain evolution code and simulated the formation of craters over a generic region. Each crater that lands can reset a circular area that is proportional to the surface area of the crater. The reset area depends on the impact velocity. For illustrative purposes, we assume all impacts occurred at the same velocity. Impacts are randomly drawn from an exponential temporal decay curve (such as that of Fig. 4a).

Our results are shown in Fig. S2 for three different levels of cratering. For each simulation we recorded (i) the distribution of all impact times and (ii) the distribution of impact ages still surviving on the surface at the end of the simulation. In scenario 1, we find that when a few impacts take place (left-hand panels), the distributions of impact times and impact ages are fairly similar one to each other; the stochastic nature of the events tends to obscure signs of the original exponential decay. In scenario 2, when more craters are formed (middle panels), both distributions resemble the original exponential decay, although the impact age distribution shows an excess of younger events due to crater superposition. Finally, in scenario 3, where heavy crater saturation takes place (right-hand panels), the distribution of recorded ages is more like a Maxwellian distribution and is skewed toward young ages. Moreover, the destruction of unaffected terrains means we are prevented from investigating the oldest times. This scenario corresponds to the so-called "brick wall" effect expected for heavily battered terrains (e.g. 74).

Testing a range of conditions, our results suggest the HEDs and H-chondrite patterns in Figs. 1 and S1 are more likely to come from scenario 1 (relatively few ^{40}Ar - ^{39}Ar resetting impacts) than scenarios 2 or 3. This is consistent with our modeling results in the main text, where the number of high velocity impactors that hit Vesta or the HPB after 4.1 Gyr ago is relatively low, as is the spatial density of affected terrains compared to the surface area in question.

In scenario 2 (middle panels), the probability of detecting the exponential decay of the impactor population correlates with the number of ^{40}Ar - ^{39}Ar impacts in the simulation; more impacts means more sampling. This suggests that to get a “flat” age distributions like those observed, the number of resetting events sampled has to be low or that some other bias is needed.

In scenario 3 (right panels), we produce a pseudo-“brick wall” run. Nearly all of the original terrain has decimated by impacts. This run shows the difficulty this scenario has in reproducing the observed HED and H-chondrite age distributions from Fig. 1; one can readily find ^{40}Ar - ^{39}Ar impact ages 3.5-4.1 Gyr ago, but at the expense of the most ancient ^{40}Ar - ^{39}Ar ages.

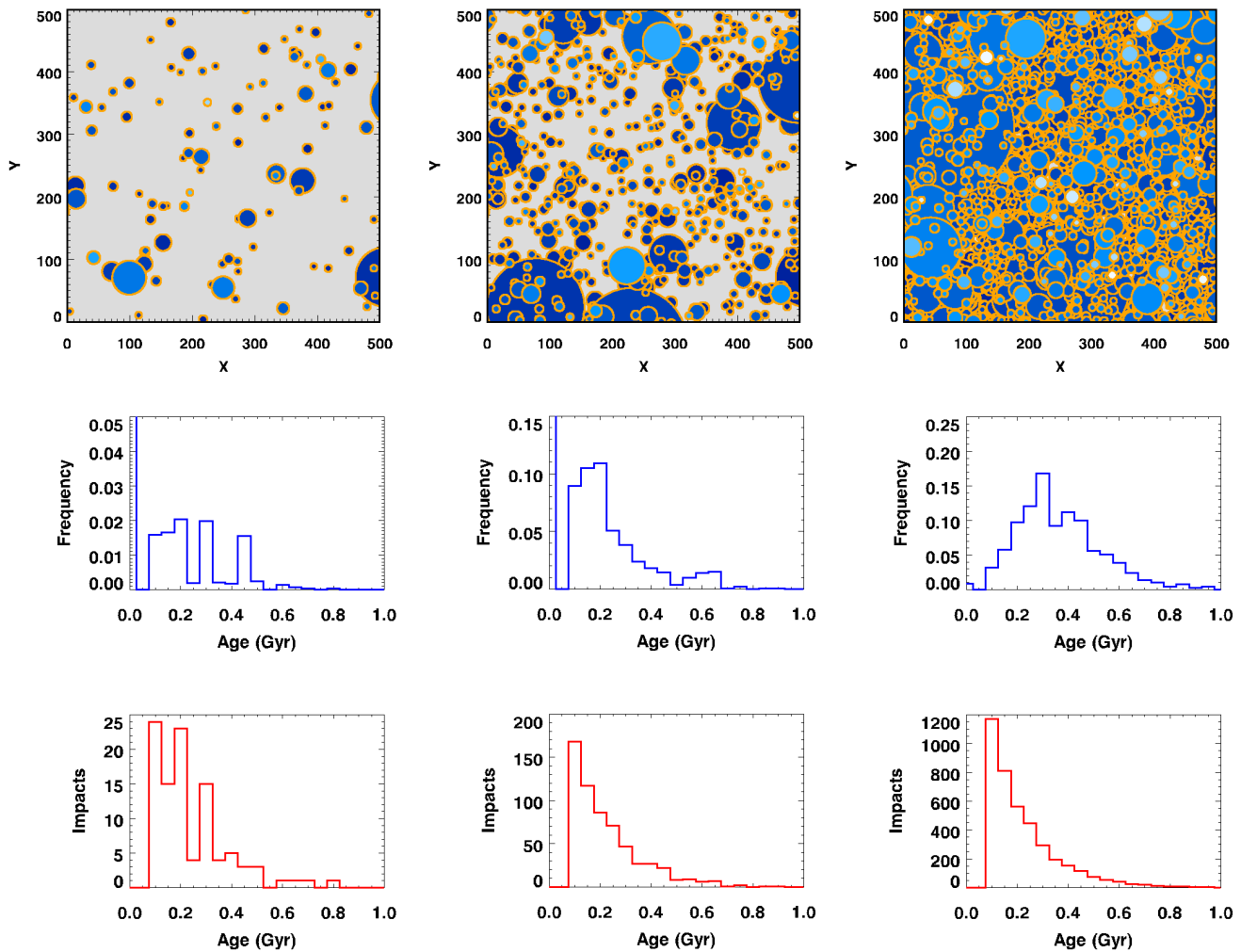


Figure S2. Results of our terrains evolution code. The upper panels are snapshots of the end of the simulations (arbitrary units). The simulations have 100, 600, 4000 craters from left to right, respectively. Circles indicate the reset area for each impact, and they are color-coded from older (dark blue) to younger (light blue) events. The distributions correspond to the impact times (red curve) and recorded impact ages at the end of the simulations (blue curve). We set the background grey area to an age of $t=0$ Gyr, while the impact flux starts at $t=0.1$ Gyr.

Note that the simulations reported in Fig. S2 assumed all impacts produce ^{40}Ar - ^{39}Ar reset ages. In a more realistic simulation, we would also include the destructive effects of non-resetting or “normal” collisions, which make up the majority of all impacts striking our asteroid's surface. Normal impacts should (i) redistribute, (ii) erode, and (iii) destroy rocks with ^{40}Ar - ^{39}Ar ages. This should create a bias favoring younger rocks, with the strength of the bias dependent on the relative (and unknown) efficiencies of (i)-(iii). Accordingly, this would provide another means for flattening the ^{40}Ar - ^{39}Ar age distributions away from an exponential.

Interestingly, the heavily cratered terrains in the northern hemisphere of Vesta are close to or possibly in crater saturation (36). Assuming Rheasilvia terrains had a similar spatial density of craters prior to the basin's formation, this could indicate that non-resetting impacts did not significantly destroy the rocks with ^{40}Ar - ^{39}Ar reset ages.

4. Hydrocode simulations of impact heating.

We used the hydrocode iSALE coupled with the ANEOS (78) equation of state for basalt to model crater formation and shock heating of target material on Vesta for impacts at different velocities. We assumed a half-space target with the gravity of Vesta. iSALE is based on the original two-step Simplified Arbitrary Lagrangian Eulerian (SALE) hydrocode (79) and has been developed by several authors (for a brief description of the history of development of the code see 46). The code is well tested against laboratory experiments and other hydrocode simulations (80). We used a tracer (massless) particle technique to record maximum shock compression which allow us to calculate the volume of material shock-heated to or above the reference temperature (Fig. S3). We used in all models a resolution of 40 cells per projectile radius (40 CPPR) which has been shown in previous studies to be sufficient (error < 10%) to determine the volume of material heated to a certain temperature (81). Simulations were run until the final craters were formed. We assume a simple strength model according to a Drucker-Prager model where shear strength Y is a linear function of pressure P : $Y = \min(Y_c + fP, Y_{\max})$, where Y_c is cohesion at zero pressure ($Y_c = 70$ KPa), f is the coefficient of friction ($f = 0.7$), and Y_{\max} is the maximum shear strength at infinite pressure ($Y_{\max} = 1.5$ GPa). However, it is assumed that shear strength has only a minor effect on shock decay and, thus, shock heating of the target. We neglect porosity in our models because HEDs have low porosity (<15%; 82); however, substantial porosity may increase the volume of material heated to a given temperature (81). Note, our simplified 2D approach to approximate an actually 3D problem is only accurate to some degree; however, the approach has been used in several studies before (the effect of impact angle on shock heating has been studied, for instance, in 33,83).

We also tracked the location of the heated material (Fig. S3). For $V = 7$ km/s, all the material heated above 1000 K is ejected from the crater, while for $V = 14, 21, 28$ km/s, about half of the heated material goes in the ejecta blanket, with the rest left at the bottom of the crater. This indicates that under the right conditions, ^{40}Ar - ^{39}Ar reset can occur both in the ejecta blanket and in the crater floor. The cooling time of the two regions, however, may differ, with hot ejecta often spread over a larger area than that of a crater floor. Thus, being all other parameters the same, the ejecta outside the crater should cool down more rapidly than the crater floor.

Finally, we briefly investigated with dedicated simulations the effects of the impactor size to the post-impact temperature and pressure profiles finding that they scale almost linearly with depth (see Fig. S3).

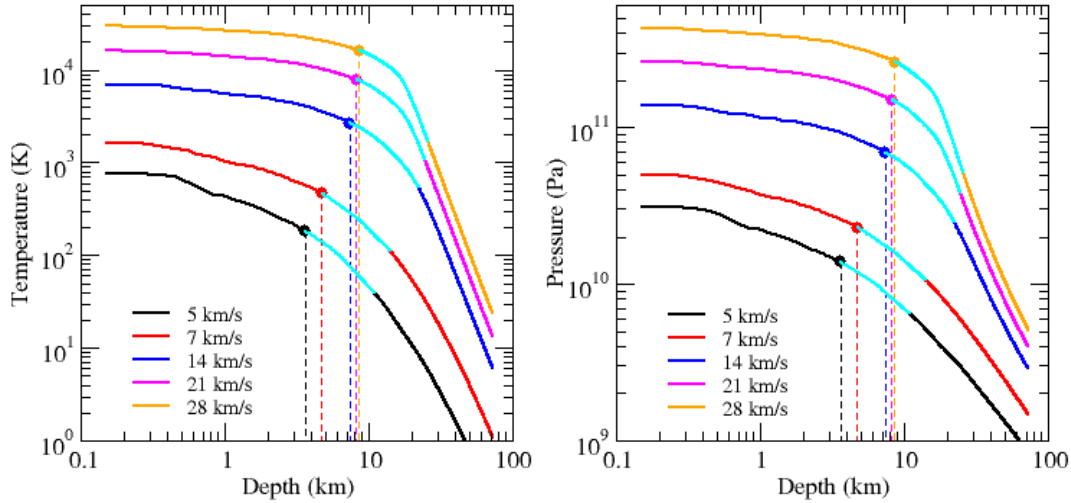


Figure S3. Post-impact temperature and pressure profiles obtained via iSALE. The curves are computed for a 10 km projectile hitting Vesta at different impact velocities V_{sim} . Impacts are simulated at 90 deg, and the effect of the most likely impact angle of 45 deg has been approximated by assuming V_{sim} is the vertical component of the impact velocity V (83). The impact velocity (V) used in our simulations is shown in the panels. Vertical dashed lines indicate the excavation depth (computed as $1/3^{rd}$ of the transient depth, 84). Cyan lines highlight the regions comprised between the excavation and transient depth, corresponding to material compacted at the bottom of the crater. Note that the depth scales almost linearly with the impactor's diameter.

5. Impact velocities of asteroids that can strike Vesta and the Moon.

In Fig. S4, we show a comparison between the mean impact velocities of objects capable of striking the Moon vs. those that can hit Vesta. We find that most objects that can hit Vesta with mean impact velocities $V > 10$ km/s can also strike the Earth-Moon system. As discussed in the main text, this may explain why the ^{40}Ar - ^{39}Ar ages of the HEDs and H-chondrites share certain similarities with those ^{40}Ar - ^{39}Ar ages derived from ancient lunar samples brought back by the Apollo astronauts as well as impact melt clasts found in lunar meteorites.

The full impact velocity distribution of asteroids capable of striking Vesta before and after late giant planet migration (assumed to be at 4.1 Gyr ago) is shown in Fig. S5. The distributions look similar to one another because the vast majority of all impacts on Vesta between 3.5-4.55 Gyr ago come from asteroids residing in the main asteroid belt. The main difference is found in the high velocity tail produced after late giant planet migration, when interactions with resonances have pushed many impactors out of the main belt and onto planet-crossing orbits.

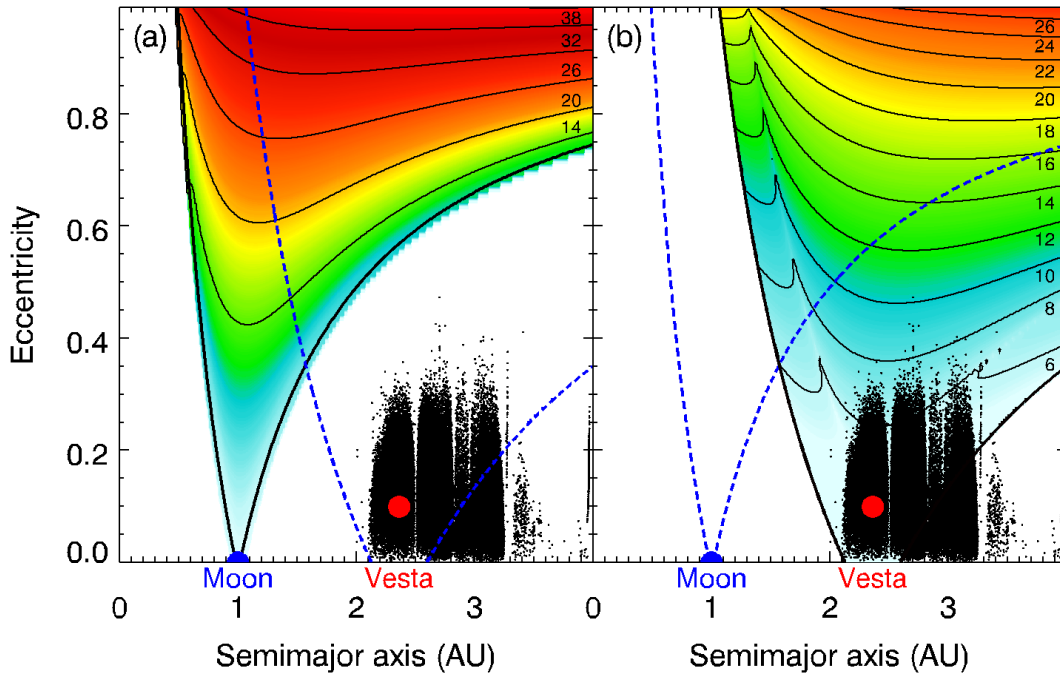
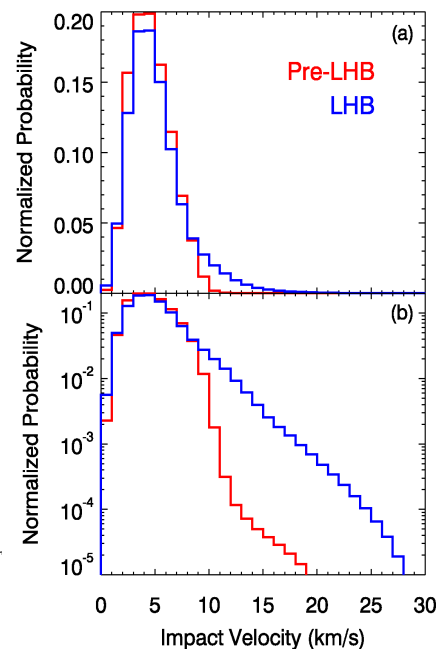


Figure S4. Impact velocity contour plots as a function of semimajor axis a and eccentricity e for objects striking the Moon and Vesta. (a) Using the methods described in (28), we computed the impact velocity distributions for a grid of test bodies in (a, e, i) space and the Moon. Here the test bodies were given $i = 10$ deg. The contours represent the mean impact velocities (units of km/s). The dashed blue lines represent the (a, e) parameters needed to reach a Vesta-crossing orbit. The black dots represent about hundred thousand of main belt asteroids in proper (a, e) . Vesta is the red dot. (b) For comparison, we show the impact velocity contours with Vesta from Fig. 3. These results indicate that most bodies capable of striking Vesta and the Moon at the same time end up either world at $V > 10$ km/s, though impact velocities on the Moon are generally higher than those on Vesta.

Figure S5. The impact velocity distributions of asteroids hitting Vesta before and after late giant planet migration at 4.1 Gyr ago, often referred to as the late heavy bombardment (LHB). The plots were calculated according to the description in the Methods section and the caption of Fig. 4. The red and blue curves correspond to the combined impact velocity distributions found between primordial main belt asteroids and Vesta for 4.1-4.55 Gyr ago (Pre-LHB) and 3.5-4.1 Gyr ago (LHB). The (a) and (b) plots are the same except for the y-axis, which is linear and log, respectively. The plots have been normalized so the sum under them is 1. The mean velocities of the pre-LHB and LHB distributions are 4.67 and 5.23 km/s, respectively. These values are similar because most impacts come from asteroids residing on stable orbits within the main belt zone. The main differences between the red and blue plots is at $V > 10$ km/s; 0.2% and 11% of all projectiles hit at these velocities, respectively.



References:

48. Bouvier, A.; Wadhwa, M. The age of the Solar System redefined by the oldest Pb-Pb age of a meteoritic inclusion. *Nature Geoscience* 3, 637-641 (2010).
49. Bennett, Marvin E., III & McSween, Harry Y., Jr. Revised model calculations for the thermal histories of ordinary chondrite parent bodies. *Meteoritics* 31, 783-792 (1996).
50. Tieloff, M.; Jessberger, E.K.; Herrwerth, I., et al. Structure and thermal history of the H-chondrite parent asteroid revealed by thermochronometry. *Nature* 422, 502-506 (2003).
51. Kleine, T., Touboul, M., van Orman, J.A., et al. Hf-W thermochronometry: Closure temperature and constraints on the accretion and cooling history of the H chondrite parent body. *Earth Planet. Sci. Lett.* 270, 106–118 (2008).
52. Rubin, A.E. Pouring 'Cold Water' on Hot Accretion. *Meteoritics* 30, p. 568 (1995).
53. Bischoff, A.; Scott, E.R.D.; Metzler, K.; Goodrich, C.A. Nature and Origins of Meteoritic Breccias. *Meteorites and the Early Solar System II*, D. S. Lauretta and H. Y. McSween Jr. (eds.), University of Arizona Press, Tucson, 943 pp., 679-712 (2006).
54. Benedix, G.K.; Ketcham, R.A.; Wilson, L. et al. The formation and chronology of the PAT 91501 impact-melt L chondrite with vesicle metal sulfide assemblages. *Geochimica et Cosmochimica Acta* 72, 2417-2428 (2008).
55. Scott, E.R.D. Metallographic Cooling Rates of H Chondrites and the Structure of Their Parent Asteroid. *Meteoritics & Planetary Science* 38, Supplement, abstract no.5293 (2003).
56. Scott, E.R.D. Meteoritic Constraints on Collision Rates in the Primordial Asteroid Belt and Its Origin. 35th Lunar and Planetary Science Conference, Texas, abstract no.1990 (2004).
57. Hopkins, M.D.; Mojzsis, S.J. Early Thermal Events in the HED Parent Body (4 Vesta) Recorded in Zircon U-Th-Pb Depth Profiles from Millbillillie Brecciated Eucrite. Workshop on the Early Solar System Bombardment II, held in Houston, Texas. LPI Contribution No. 1649, p.30-31 (2012).
58. Scott, E.R.D. & Bottke, W.F. Impact histories of angrites, eucrites, and their parent bodies. *Meteoritics & Planetary Science* 46, 1878-1887 (2011).
59. Norman, M.D.; Duncan, R.A.; Huard, J.J. Identifying impact events within the lunar cataclysm from ^{40}Ar - ^{39}Ar ages and compositions of Apollo 16 impact melt rocks. *Geochimica et Cosmochimica Acta* 70, 6032-6049 (2006).
60. Shuster, D.L.; Balco, G.; Cassata, W.S.; Fernandes, V.A.; Garrick-Bethell, I.; Weiss, B.P. A record of impacts preserved in the lunar regolith. *Earth and Planetary Science Letters* 290, 155-165 (2010).
61. Marvin, U.B.; Lindstrom, M.M.; Bernatowicz, T.J.; Podosek, F.A.; Sugiura, N. The composition and history of breccia 67015 from North Ray Crater. *JGR* 92, E471-E490 (1987).
62. Bernatowicz, T.J.; Lindstrom, M.M.; Podosek, F.A. ^{40}AR - ^{39}AR Ages of Apollo 16 North Ray

Crater Rocks and Dimict Breccias. LPS XVII, 42-43 (1986).

63. Jessberger, E.K.; Huneke, J.C.; Podosek, F.A.; Wasserburg, G.J. High resolution argon analysis of neutron-irradiated Apollo 16 rocks and separated minerals. Lunar Science Conference, 5th, Houston, Tex., Proceedings. Volume 2. (A75-39540 19-91) New York, Pergamon Press, Inc., 1419-1449 (1974).

64. Schaeffer, O.A. & Husain, L. Early lunar history: Ages of 2 to 4 mm soil fragments from the lunar highlands. Proceedings of the Lunar Science Conference, vol. 4, p.1847 (1973).

65. Huneke, J.C.; Jessberger, E.K.; Podosek, F.A.; Wasserburg, G.J. $^{40}\text{Ar}/^{39}\text{Ar}$ measurements in Apollo 16 and 17 samples and the chronology of metamorphic and volcanic activity in the Taurus-Littrow region. Proceedings of the Lunar Science Conference, vol. 4, p.1725 (1973).

66. Maurer, P.; Eberhardt, P.; Geiss, J.; Grogler, N.; Stettler, A.; Brown, G.M.; Peckett, A.; Krahenbuhl, U. Pre-Imbrian craters and basins - Ages, compositions and excavation depths of Apollo 16 breccias. *Geochimica et Cosmochimica Acta* 42, 1687-1720 (1978).

67. Cohen, B.A.; Swindle, T.D.; Taylor, L.A.; Nazarov, M.A. ^{40}Ar - ^{39}Ar Ages from Impact Melt Clasts in Lunar Meteorites Dhofar 025 and Dhofar 026. 33rd Annual Lunar and Planetary Science Conference, Houston, Texas, abstract no.1252 (2002).

68. Cohen, B.A.; Swindle, T.D.; Kring, D.A. Geochemistry and ^{40}Ar - ^{39}Ar geochronology of impact-melt clasts in feldspathic lunar meteorites: Implications for lunar bombardment history. *Meteoritics & Planetary Science* 40, p.755 (2005).

69. Fernandes, V.A.; Burgess, Ray; Turner, Grenville. Laser argon-40-argon-39 age studies of Dar al Gani 262 lunar meteorite. *Meteoritics & Planetary Science* 35, 1355-1364 (2000).

70. Fernandes, V.A.; Anand, M.; Burgess, R.; Taylor, L.A. Ar-Ar Studies of Dhofar Clast-rich Feldspathic Highland Meteorites: 025, 026, 280, 303. 35th Lunar and Planetary Science Conference, League City, Texas, abstract no.1514 (2004).

71. Daubar, I.J.; Kring, David A.; Swindle, T.D.; Jull, A.J.T. Northwest Africa 482: A crystalline impact-melt breccia from the lunar highlands. *Meteoritics & Planetary Science* 37, 1797-1813 (2002).

72. Warren, P.H. Lunar and martian meteorite delivery services. *Icarus* 111, 338-363 (1994).

73. Gladman, B.J.; Burns, J.A.; Duncan, M.J.; Levison, H.F. The dynamical evolution of lunar impact ejecta. *Icarus* 118, 302-321 (1995).

74. Hartmann, W.K. Megaregolith evolution and cratering cataclysm models--Lunar cataclysm as a misconception (28 years later). *Meteoritics & Planetary Science* 38, 579-593 (2003).

75. Bottke, W.F., D. Durda, D. Nesvorny, R. Jedicke, A. Morbidelli, D. Vokrouhlicky, and H. Levison. The origin and evolution of stony meteorites. In *Dynamics of Populations of Planetary Systems* (Z. Knezevic, A. Milani, Eds). IAU Colloquium 197, 357-374 (2005).

76. Rubin, A.E.; Bottke, W.F. On the origin of shocked and unshocked CM clasts in H-chondrite regolith breccias. *Meteoritics & Planetary Science* 44, 701-724 (2009).

77. Gaffey, M.J. & Gilbert, S.L. Asteroid 6 Hebe: The probable parent body of the H-Type ordinary chondrites and the IIE iron meteorites. *Meteoritics & Planetary Science* 33, 1281-1295 (1998).
78. Pierazzo, E., N.A. Artemieva, and B.A. Ivanov, Starting conditions for hydrothermal systems underneath Martian craters: Hydrocode modeling, in *Special Paper 384: Large Meteorite Impacts III*, edited by T. Kenkmann, F. Horz, and A. Deutsch, pp. 443-457, Geological Society of America, Boulder, Co., 2005.
79. Amsden, A.A.; Ruppel, H.M.; Hirt, C.W. SALE: a simplified ALE computer program for fluid flow at all speeds. Technical Report LA-8095. Los Alamos Scientific Lab., NM (USA), pp.105 (1980).
80. Pierazzo E., and 13 co-authors. Validation of numerical codes for impact and explosion cratering: impact on strengthless and metal targets. *Meteoritics & Planetary Science* 43, 1917-1938 (2008).
81. Wünnemann K., Collins G.S., and Osinski G.R. Numerical modelling of impact melt production in porous rocks. *Earth and Planetary Science Letters* 269, 530-539 (2008).
82. Britt, D.T.; Consolmagno, G.J. Stony meteorite porosities and densities: A review of the data through 2001. *Meteoritics & Planetary Science* 38, 1161-1180 (2003).
83. Pierazzo, E. & Melosh, H.J. Melt Production in Oblique Impacts. *Icarus* 145, 252-261 (2000).
84. Melosh, H.J. *Impact cratering: A geologic process*. New York, Oxford University Press (Oxford Monographs on Geology and Geophysics, No. 11), 253 p., (1989).